Radiation and Absorption Properties of Gold Nanodipoles in Transmitting Mode

K. Q. Costa, V. Dmitriev, T. L. T. Santos, N. W. P. Souza, J. L. Souza, and G. L. Silvano

***Abstract*—This paper presents an analysis of radiation and absorption properties of cylindrical gold nanodipoles in the transmitting mode. The conventional antenna theory and the linear method of moments are used for the theoretical analysis of these antennas in the near-infrared and lower optical frequencies (100−500THz). Radiation and absorption parameters, such as input impedance, efficiency, radiation and loss resistance are calculated in function of frequency for different dipole's lengths and radii. The presented results can be useful to design efficient nanodipoles and to perform the input impedance matching of these antennas with plasmonic optical transmission lines.**

***Keywords*—Optical antennas, cylindrical dipoles, plasmonics, radiation.**

I. INTRODUCTION

Optical antennas are metal nanostructures used to transmit or receive optical fields [1]-[2]. This definition is similar to that of conventional radio frequency (RF) and microwave antennas. The main difference between these two regimes (RF-microwave and optical) occurs due to physical properties of the metals at optical frequencies where they cannot be considered as perfect conductors because of the plasmonic effects [3]. Recently comprehensive reviews on optical antennas have been presented in [4]-[5]. In these works, the authors described recent developments, antenna parameters, applications, future trends and challenges.

A potential application of optical antennas is to provide a good matching between guided plasmonic waves and radiated fields, and vice versa. One example of enhancement of the reception of propagating surface plasmons using nanodipoles placed in front the waveguide's end aperture is given in [6]. Another example is enhancement of the near field of an aperture optical fiber probe by using a monopole near this aperture [7]. Also, a nanodipole can provide a better enhancement and confinement of the radiated fields of a semiconductor laser diode [8]. In all these examples, the dimensions and resonances of the antennas were optimized to improve the energy transfer between the guided and radiated fields. These problems can be viewed as a classical input impedance matching design, in analogy with the theory of RF- and microwave antennas.

To take advantage of the well established input impedance matching techniques of RF-microwave antennas, it is necessary to extend the antenna theory to the optical domain. To do this, plasmonic waveguides and nanoantennas can be represented by equivalent optical transmission lines (OTL) and impedances, respectively. In this way, a plasmonic OTL based on array of nanoparticles, acting as lumped nanocircuit elements, have been proposed in [9]. Other examples of OTL and equivalent circuit analysis can be found in [10]-[11]. An optical nanocircuit composed by a receiving and an emitting nanoantenna connected by a two-wire OTL is presented in [12]. In this paper, the authors performed the input impedance matching varying de length of the nanodipoles.

Input impedances of isolated nanoantennas in the transmitting mode were investigated in [13]-[16]. In [13], the input impedance of silver linear nanodipoles with different length and loading is analyzed. The effect of different materials and sizes on the input impedance of linear nanodipoles is presented in [14]. The peculiar properties of loop nanoantennas are presented in [15]. Plasmonic folded dipole nanoantennas with better radiation efficiency are investigated in [16]. In all these works, the principal objective is to analyze the input impedance and the resonance properties of nanoantennas, and minor attention has been given to the absorptive and efficiency properties of the nanoantennas, which is very important to design efficient plasmonic optical nanocircuits.

In this paper, we present a radiation and absorption analysis of gold linear nanodipoles in the transmitting mode. The conventional antenna theory and the linear method of moments with sinusoidal basis functions and equivalent surface impedance are used for the theoretical analysis in the near-infrared and lower optical frequencies (100−500THz). Radiation and absorption parameters, such as input impedance, loss and radiated power, efficiency, loss and radiation resistance are calculated in function of frequency for different dipole's length and radius. Our results give some useful conclusions for design efficient nanodipoles and to make the input impedance matching of these antennas with OTLs. The following sections present the theoretical model, results, and conclusions.

II. THEORETICAL MODEL

To analyze linear nanodipoles we use the method of moments (MoM) approximation with sinusoidal basis functions and equivalent surface impedance [17]. Fig. 1 shows the geometry of the original problem, the equivalent moment method and circuit models of the nanodipole. In this figure, L is the length of the arms, d is the nanodipole gap, and a is the radius. The total length of this antenna is L_t=2L+d.

In the radiation problem of the Fig. 1, the gold material of the antenna is represented by the Lorentz-Drude model for the complex permittivity $\varepsilon_1 = \varepsilon_0\varepsilon_{r1}$ [17], where

$$\varepsilon_{r1} = \varepsilon_\infty - \frac{\omega_{p1}^2}{\omega^2 - j\Gamma\omega} + \frac{\omega_{p2}^2}{\omega_0^2 - \omega^2 + j\gamma\omega} \qquad (1)$$

Karlo Q. da Costa, Victor Dmitriev, Thais L. T. Santos, Nadson W. P. Souza, Janilson L. de Souza, Gustavo L. Silvano, 1Department of Electrical Engineering, Campus of Tucuruí, Federal University of Para, Tucuruí-PA, Brazil, E-mails: karlo@ufpa.br,victor@ufpa.br. This work was partially supported by the Brazilian agency CNPq.

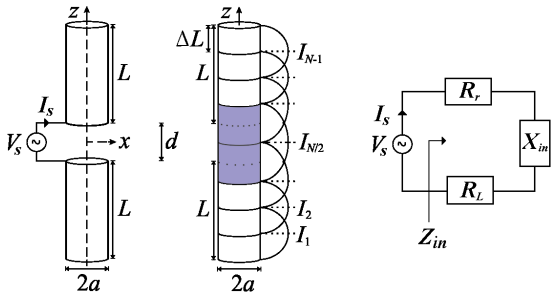

Fig. 1. Geometry of nanodipole: original problem (left), method of moments model (midlle), equivalent circuit model (right).

being: ε_∞=8, ω_{p1}=13.8×10^{15}s^{-1}, Γ=1.075×10^{14}s^{-1}, ω_0=2πc/λ_0, λ_0=450nm, ω_{p2}=45×10^{14}s^{-1}, and γ=9×10^{14}s^{-1}. This model is a good approximation for the wavelengths λ>500nm. The losses in metal are described by surface impedance Z_s. This surface impedance can be obtained approximately by considering cylindrical waveguide with the mode TM$_{01}$. In this case, the surface impedance is given by

$$Z_s = \frac{TJ_0(Ta)}{2\pi aj\omega\varepsilon_1 J_1(Ta)}, \quad T = k_0\sqrt{\varepsilon_{r1}}, \quad k_0 = \omega\sqrt{\mu_0\varepsilon_0}\,. \tag{2}$$

The boundary condition for the electric field satisfied at the surface's conductor is $(\bar{E}_s + \bar{E}_i)\cdot\bar{a}_l = Z_s I$, where a_l is a unitary vector tangential to the surface of the metal, E_s is the scattered electric field due the induced linear current I on the conductor, E_i the incident electric field from the voltage source (Fig. 1), and I is the longitudinal current in a given point of the nanodipole.

The integral equation of the scattered field along the length l of the nanodipole is given by

$$\bar{E}_s(\bar{r}) = \frac{1}{j\omega\varepsilon_0}\left[k_0^2\int_l \bar{I}g(R)dl' + \int_l \frac{dI}{dl'}\nabla g(R)dl'\right], \tag{3}$$
$$g(R) = \frac{e^{-jk_0R}}{4\pi R}, \quad R = |\bar{r}-\bar{r}'|, \quad \bar{I} = I\,\bar{a}_l\,.$$

The numerical solution of the problem formulated by (1)-(3), is performed by linear MoM as follows. Firstly, we divide the total length L_t=2L+d in N=2N_a+2 total straight segments, where N_a is the number of segments in L−0.5d, with size ΔL=(L−0.5d)/N_a (white segments in Fig. 1), and two segments in the middle with size ΔL=d (gray segments in Fig. 1). Later, the current in each segment is approximated by sinusoidal basis functions. The expansion constants I_n are shown in Fig. 1 where each constant define one triangular sinusoidal current. To determine these constants, we use N−1 rectangular pulse test functions with unitary amplitude and perform the conventional testing procedure. The following linear system of equations is obtained

$$V_m = Z_s I_m \Delta_m - \sum_{n=1}^{N-1} Z_{mn} I_n\,, \quad m=1, 2, 3, \ldots, N-1 \tag{4}$$

where Z_{mn} is the mutual impedance between sinusoidal current elements m and n, Δ_m=1/2[ΔL_m+ΔL_{m+1}], and V_m is only non zero in the middle (m=N/2), where $V_{N/2}$=V_s. The solution of (4) gives the current along the dipole, and the input current I_s. For V_s=1V, the input impedance is Z_{in}=1/I_s=(R_r+R_L)+jX_{in}, where R_r, R_L, and X_{in} are the radiation resistance, loss resistance, and input reactance, respectively. The total input power is P_{in}=0.5Re($V_s I_s^*$)=0.5(R_L+R_r)$|I_s|^2$=P_r+P_L, P_r is the radiated power and P_L the loss power dissipated at the antenna's surface. This later is calculated numerically by

$$P_L = 0.5\,\mathrm{Re}(Z_s)\sum_{n=1}^{N-1}|I_n|^2\Delta_n\,. \tag{5}$$

The radiated power can be obtained by P_r=P_{in}−P_L, and the resistances R_r=2P_r/$|I_s|^2$ and R_L=2P_L/$|I_s|^2$. The radiation efficiency is calculated by e_r=P_r/P_{in}= P_r/(P_r+P_L)=R_r/(R_r+R_L).

III. Results and Comments

A. Numerical Example

This section presents the numerical analysis of an example nanodipole with L=220nm, a=10nm, and d=20nm. The simulations of this nanodipole using the theory presented in the previous section, were performed for N_a=11 (N=24). With this discretization the convergence criteria that we use of min(ΔL)/a≥1 is satisfied. In this case, we have min(ΔL)/a=1.9.

The calculated input impedance Z_{in} is shown in Fig. 2. This figure also presents the result simulated by the Comsol software. We observe a good agreement of the results in the range 100−400THz. In general, for higher optical frequencies F>400THz, the surface impedance approximation (2), of the linear method of moment used here, is not valid [18]. In this case, the contribution of the transversal current in the nanodipole will be significant and it should be taken into consideration [19].

The data of Fig.2 show that the Z_{in} curve and the resonances of nanodipoles are similar to the conventional RF-microwave dipoles. The difference is that the resonances of nanodipoles are shifted for lower frequencies, because the *effective* wavelength of the material is smaller than the external wavelength. This behavior is known as *scaling rule* for optical antennas [20]-[21].

The first four resonances of this nanodipole defined by X_{in}=0 are: F$_{\lambda/2}$=136THz (first short-circuit resonance), F$_\lambda$=221THz (first open-circuit resonance), F$_{3\lambda/2}$=330THz (second short-circuit resonance), and F$_{2\lambda}$=379THz (second open-circuit resonance). These resonances are of type short or open circuit; it depends on the form of their current distributions (Fig. 3).

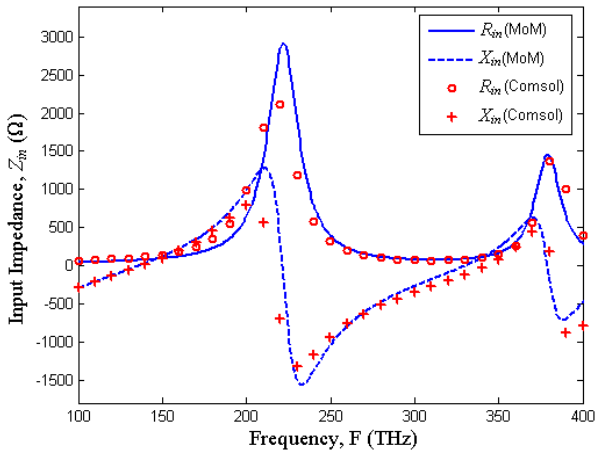

Fig. 2. Input impedance of nanodipole with L=220nm, a=10nm, and d=20nm. The simulation with MoM was made for N_a=11 (N=24).

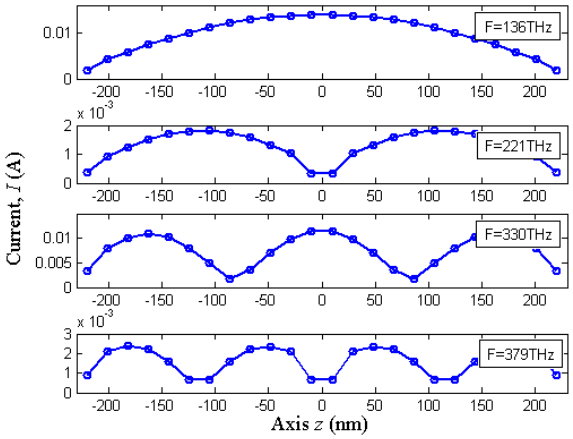

Fig. 3. Current distribution along nanodipoles at resonances.

In Fig. 4, we present the loss power (P_L), radiated power (P_r), loss resistance (R_L), and radiation resistance (R_r) versus frequency. Fig. 5 shows the directivity (D), gain (G) and radiation efficiency (e_r) of the nanodipole versus frequency. The parameters D and G were calculated in the far field zone in the x direction (Fig. 1). The inset in this figure presents the radiation diagram of gain for different resonant frequencies.

We observe in these figures that the maximum of P_L and P_r occurs at the short-circuit resonances, and the maximum of R_L and R_r occur at the open-circuit resonances. The values of the radiation efficiency are small when compared with those for RF-microwave antennas. This is due the high losses of the metal in optical frequencies. The maximum of the radiation efficiency of this nanodipole is e_r=0.39, and it occurs at the open-circuit resonance F_λ=221THz. This means that the maximum efficiency and maximum input power are in different frequencies. Also, maximum efficiency and better input impedance matching of this nanodipole with a given OTL, in general, are in different frequencies. This happen because the characteristic impedance of an OTL not necessary matches with the input impedance of the nanodipole at maximum efficiency [12].

The maximum gain of this nanodipole is G=−2.27dB, and it occurs at maximum efficiency (Fig. 5) because the directivity is nearly constant, about D=1.5 (≈1.9dB). The shape of the radiation diagram of gain of this nanodipole in the plane xz is approximately the same as that of a small dipole.

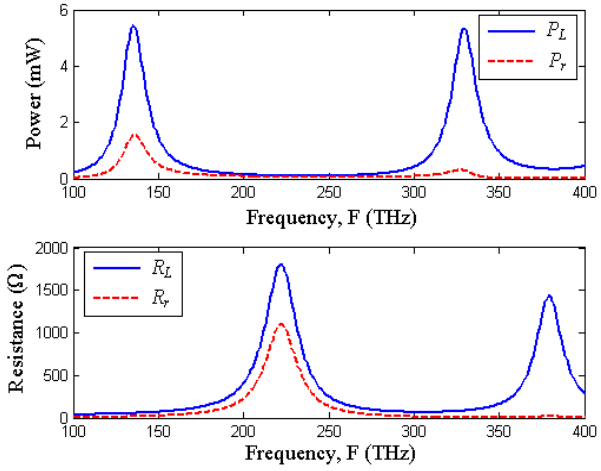

Fig. 4. Loss power (P_L), radiated power (P_r), loss resistance (R_L), and radiation resistance (R_r) versus frequency.

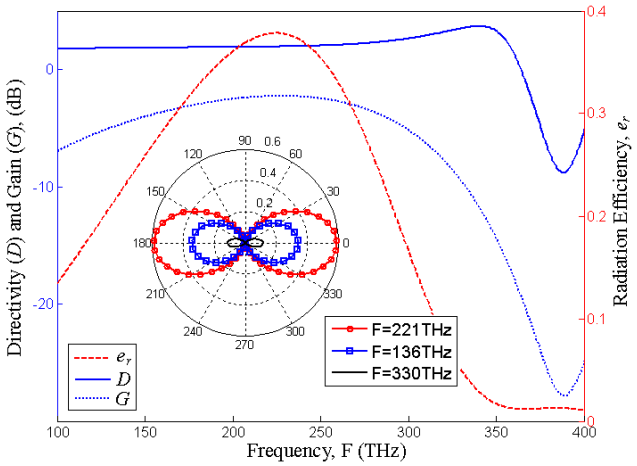

Fig. 5. Directivity (D), gain (G) and radiation efficiency (e_r) of the nanodipole versus frequency.

B. *Parametric Analysis*

This section presents a parametric analysis of nanodipoles with different values of the arm length L and radius a. The objective is to investigate the variation of the radiation and absorption properties of nanodipoles with different sizes.

Figs. 6-7 show the variation of the input impedance for L=100, 125, 150, and 175nm, for a=10 and 20nm, respectively.

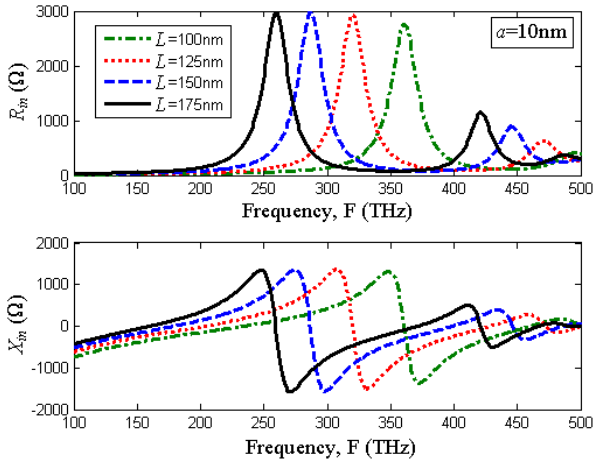

Fig. 6. Input impedance of the nanodipole with L=100, 125, 150, and 175nm, for a=10nm.

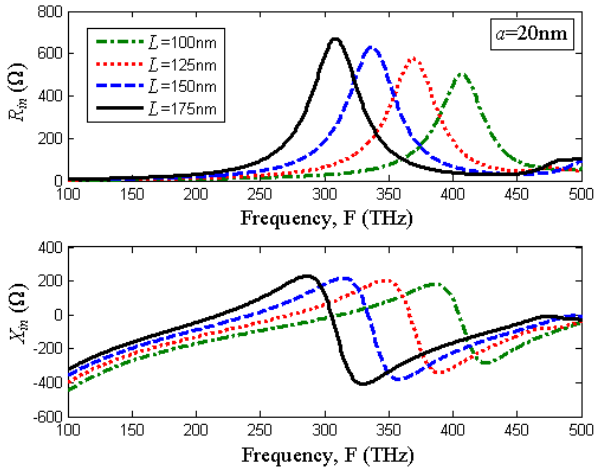

Fig. 7. Input impedance of the nanodipole with L=100, 125, 150, and 175nm, for a=20nm.

We see in this figures that with increasing of L and fixed radius, the resonances of the dipole are shifted to lower frequencies, and for increasing of a, for fixed L, the resonances are increased. This dependence of the resonances is similar to the variation of the resonances of nanorods illuminated by a plane wave [20]-[21], where one observes a linear dependence of the resonant wavelengths λ_{res} with L, and with variable inclination of the linear curve for different values of a. These figures also show that the widths of the R_{in} curves, around the open-circuit resonances, are broader for larger values of a. In other words, the impedance bandwidth is increased for larger a. This result is similar for the case of RF-microwave broadband dipoles with smaller aspect ratio L/a. We also notice that with fixed a the values of R_{in} are increased for larger L.

Figs. 8-9 present the variation of the loss power (P_L) and radiated power (P_r) for different L and a, respectively. The position of the maximum power in these curves occur at the correspondent short-circuit resonances of the input impedances shown in Figs. 6-7. This was observed in the example of the previous section (Figs. 2 and 4). Also, the maximum values of P_L and P_r are reduced with increasing the arm length L. However, for higher values of a, with fixed L, P_L is reduced and P_r is increased. To take a better physical understanding of these results, it is important to analyze the loss and radiation resistance and the equivalent circuit of Fig. 1.

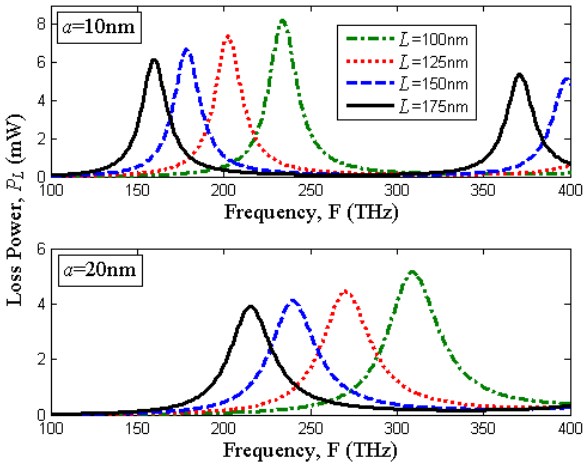

Fig. 8.

Fig. 9. Loss power P_L for nanodipoles with different values of L=100, 125, 150, and 175nm, and a=10 and 20nm.

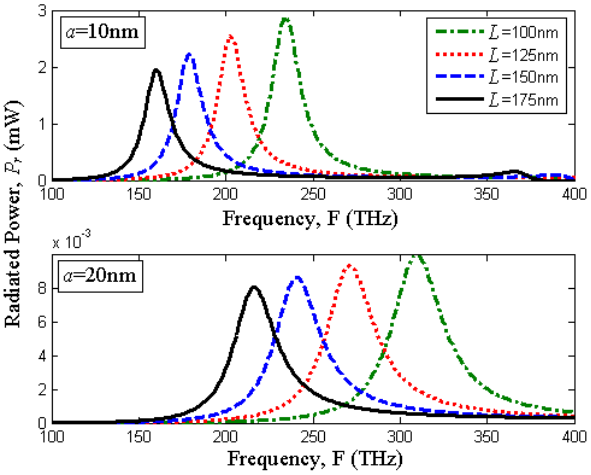

Fig. 10. Radiated power P_r for nanodipoles with different values of L=100, 125, 150, and 175nm, and a=10 and 20nm.

Figs. 10-11 present the dependence on L and a of loss resistance (R_L) and radiation resistance (R_r). We observe that the maximum values of R_L and R_r are in the open-circuit resonances of the correspondent input impedance (Figs. 6-7), like observed in the example of Fig. 4. For increasing L, with fixed a, the curves of R_L practically are not changed, and the curves of R_r are increased. This means that the increasing of the input resistance (Figs. 6-7) is due mainly by R_r. For increasing the radius a, both resistances are reduced, but the reduction for R_L is larger than that observed for R_r. This explain the variation of P_L and P_r, for different a and fixed L, shown in Figs. 8-9. The reduction of P_L for higher values of a is due to the reduction in the surface impedance Z_s (2), which leads to a weaker plasmonic effect. This also happens for higher L, because the resonances are red-shifted [18].

The circuit analysis of these linear gold nanodipoles with different values of L and a, and using V_s=1V, the input impedance of Figs. 6-7, and the resistances of Figs. 10-11, produces the results of loss and radiated power shown in Figs. 8-9. The radiation efficiency has been calculated and the results are presented in Fig. 12. We can conclude that, in general, the radiation efficiency is increased for larger values of L and a, i.e for larger nanodipoles sizes, where the plasmonic effect is smaller.

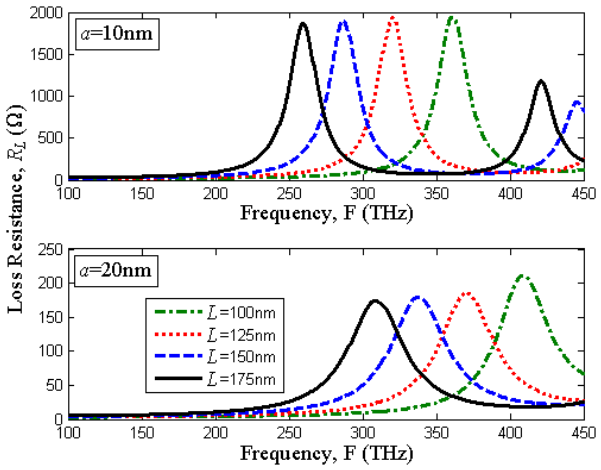

Fig. 11. Loss resistance R_L for nanodipoles with different values of L=100, 125, 150, and 175nm, and a=10 and 20nm.

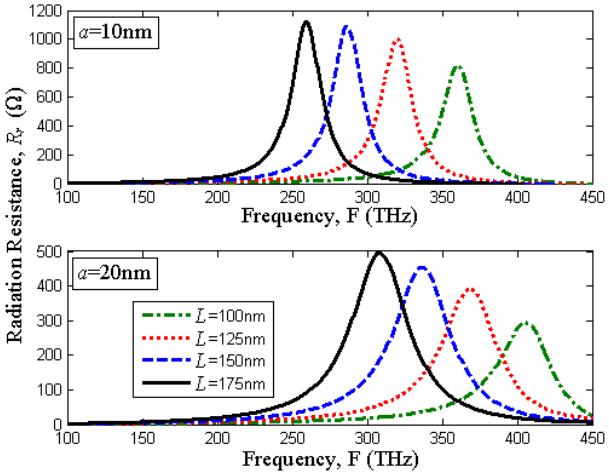

Fig. 12. Radiation resistance R_r for nanodipoles with different values of L=100, 125, 150, and 175nm, and a=10 and 20nm.

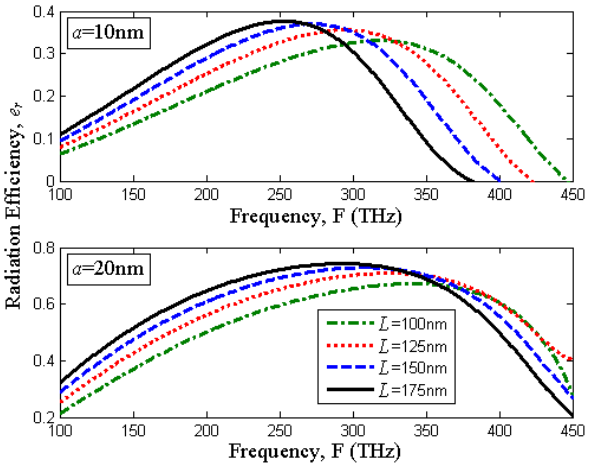

Fig. 13. Radiation efficiency (e_r) for nanodipoles with different values of L=100, 125, 150, and 175nm, and a=10 and 20nm.

IV. CONCLUSION

This paper presented a theoretical analysis of radiation and absorption properties of cylindrical gold nanodipooles in the transmitting mode. The linear method of moments with sinusoidal basis functions was used to determine the equivalent circuit model for nanodipoles with different arm length L and radius a. The equivalent circuit was used to calculate the losses, radiated power, and efficiency. We observed that the maximum radiation efficiency, for all analyzed nanodipoles, occur at the first open-circuit resonance, where the input resistance is very high. Another important result obtained is that, in general, the radiation efficiency of nanodipoles is small, but it can be increased for large values of L and a.

The analysis presented here can be useful to design efficient nanodipoles, and to make the input impedance matching of these nanodipoles with a given OTL. In future works, we shall investigate nanoantennas with different materials and geometries to optimize the input impedance and radiation efficiency.

REFERENCES

[1] R. D. Grober, et. al., "Optical antenna: towards a unity efficiency near-field optical probe", *Appl. Phys. Lett.*, v. 70, pp. 1354–1356, Mar. 1997.

[2] D. W. Pohl, "Near field optics as an antenna problem"', *Near Field: Principles and Applications*, *The second Asia-Pacific Workshop on Near Field Optics*, Beijing, China October 20–23, pp. 9–21, 1999.

[3] S. A. Maier, *Plasmonics: Fundamentals and Applications*, New York: Springer, 2007.

[4] P. Bharadwaj, et. al., "Optical antennas", *Adv.in Opt. and Photon.*, v. 1, pp. 438–483, Aug. 2009.

[5] L. Novotny, and N. V. Hulst, "Antennas for light", *Nature Photon.*, v. 5, Feb. 2011.

[6] M. Gu, et. al., "Enhancing the reception of propagating surface plasmons using a nanoantenna", *IEEE Phot. Tech. Lett.*, v. 22, N4, pp. 245–247, Feb. 2010.

[7] T. H. Taminiau, et. al., "A monopole antenna at optical frequencies: single-molecule near-field measurements", *IEEE Trans. on Ant. and Propag.*, v. 55, N11, pp. 3010–3017, Nov. 2007.

[8] E. Cubukcu, et. al., "Plasmonic laser antennas and related devices", *IEEE J. of Select. Top. in Quant. Electronics*, v. 14, N6, pp. 1448–1461, Nov. 2008.

[9] N. Engheta, "Circuits with light at nanoscales: optical nanocircuits inspired by metamaterials", *Science*, v. 317, pp. 1698–1702, Sep. 2007.

[10] H. Pahlevaninezhad, et. al., "Two-wire waveguide for terahertz", *Opt. Express*, v. 18, N7, pp. 7415–7420, Mar. 2010.

[11] Y. Choi, et. al., "Metal-insulator-metal optical nanoantenna with equivalent-circuit analysis", *Adv. Mat.*, v. 22, pp. 1754–1758, 2010.

[12] J.-S. huang, et. al., "Impedance matching and emission properties of nanoantennas in an optical nanocircuit", *Nano Lett.*, v. 9, N5, pp. 1897–1902, 2009.

[13] A. Alù, and N. Engheta, "Input impedance, nanocircuit loading, and radiation tuning of optical nanoantennas", *Phys. Rev. Lett.*, v. 101, p. 043901, Jul. 2008.

[14] F. P. G. Arquer, et. al., "Engineering the input impedance of optical nano dipole antennas: materials, geometry and excitation effect", *IEEE Trans. on Ant. And Propag.*, v. 59, N9, pp. 3144–3153, Sep. 2011.

[15] A. Locatelli, "Peculiar properties of loop nanoantennas", *IEEE Phot. J.*, v. 3, N5, pp. 845–853, Oct. 2011.

[16] H. Iizuka, et. al., "Arm-edge conditions in plasmonic folded dipole nanoantennas", *Opt. Express*, v. 19, N13, pp. 12325–12335, Jun. 2011.

[17] K. Q. Costa, and V. Dmitriev, "Numerical analysis of cylindrical nanodipoles by linear moment method", *Int. Microwave. and Opto. Conf.*, Natal – RN, Brazil, 2011.

[18] G. W. Hanson, "On the applicability of the surface impedance integral equation for optical and near infrared copper dipole antennas", *IEEE Trans. on Ant. and Propag.*, v. 54, N12, pp. 3677–3685, Dec. 2006.

[19] A. Rashid, et. al., "Scattering analysis of plasmonic nanorod antennas: a novel numerically efficient computational scheme utilizing macro basis functions", *J. of Appl. Phys.*, v. 109, p. 123109, Jun. 2011.

[20] L. Novotny, "Effective wavelength scaling for optical antennas", *Phys. Rev. Lett..*, v. 98, p. 266802, Jun. 2007.

[21] G. W. Bryant, et. al., "Mapping the plasmon resonances of metallic nanoantennas", *Nano Lett.*, v. 8, N2, pp. 631–636, Dec. 2008